



Article

Outdoor Thermal Comfort during Anomalous Heat at the 2015 Pan American Games in Toronto, Canada

Alexandria J. Herdt¹, Robert D. Brown², Ian Scott-Fleming³, Guofeng Cao⁴ ,
Melissa MacDonald⁵, Dave Henderson⁵ and Jennifer K. Vanos^{1,6,*} 

¹ Department of Geosciences, Atmospheric Science Group, Texas Tech University, Lubbock, TX 79409, USA; aherdt0725@gmail.com

² Department of Landscape Architecture and Urban Planning, Texas A&M University, College Station, TX 77843, USA; rbrown@arch.tamu.edu

³ Department of Electrical and Computer Engineering, Texas Tech University, Lubbock, TX 79409, USA; ian.scott-fleming@ttu.edu

⁴ Department of Geosciences, Geography, Texas Tech University, Lubbock, TX 79409, USA; guofeng.cao@ttu.edu

⁵ Environment and Climate Change Canada, Toronto, ON M3H 5T4, Canada; melissa.macdonald@canada.ca (M.M.); daveh@magma.ca (D.H.)

⁶ Scripps Institution of Oceanography, University of California San Diego, La Jolla, CA 92093, USA

* Correspondence: jkvanos@ucsd.edu; Tel.: +858-534-4446

Received: 20 June 2018; Accepted: 31 July 2018; Published: 18 August 2018



Abstract: Mass sporting events in the summertime are influenced by underlying weather patterns, with high temperatures posing a risk for spectators and athletes alike. To better understand weather variations in the Greater Toronto Area (GTA) during the Pan American Games in 2015 (PA15 Games), Environment and Climate Change Canada deployed a mesoscale monitoring network system of 53 weather stations. Spatial maps across the GTA demonstrate large variations by heat metric (e.g., maximum temperature, humidex, and wet bulb globe temperature), identifying Hamilton, Ontario as an area of elevated heat and humidity, and hence risk for heat-related illness. A case study of the Hamilton Soccer Center examined on-site thermal comfort during a heat event and PA15 Soccer Games, demonstrating that athletes and spectators were faced with thermal discomfort and a heightened risk of heat-related illness. Results are corroborated by First Aid and emergency response data during the events, as well as insight from personal experiences and Twitter feed. Integrating these results provides new information on potential benefits to society from utilizing mesonet systems during large-scale sporting events. Results further improve our understanding of intra-urban heat variability and heat-health burden. The benefits of utilizing more comprehensive modeling approaches for human heat stress that coincide with fine-scale weather information are discussed.

Keywords: thermal comfort; extreme heat; Pan American Games; heat stress; solar radiation

1. Introduction

1.1. Pan and Para Pan American Games (PA15 Games)

The Pan American Games are an Olympic-style competition held every four years in the year preceding the Summer Olympic Games for athletes from countries within the Americas. The Para Pan American Games are a similar competition held immediately after the Pan American Games for athletes with physical disabilities. The two competitions combined are henceforth referred to as the ‘PA15 Games’. The PA15 Games took place in Toronto, Ontario, Canada in 2015 from July 10th–26th and August 7th–15th, respectively. As with any summer sporting event, heat-related illnesses and

mortality are a risk [1]. Thus, monitoring and relaying real-time information regarding the physical environment during competition is pivotal for athlete and spectator health not only for heat but also for hazardous summer weather. Environment and Climate Change Canada (ECCC) was mandated to provide enhanced weather and air quality (AQ) monitoring for the provision of venue-specific public hazardous weather, AQ, and health alerts during the PA15 Games [2]. The current article showcases the value of weather observations for intra-urban heat variability in the Greater Toronto Area (GTA) during the summer period of 2015, and further completes a detailed case study at the Hamilton Soccer Center during a heat wave that coincided with three mass sporting events.

1.2. Urban Heat Variability and Thermal Comfort

With an expansive urban area and large population, the City of Toronto and surrounding cities prominently demonstrate urban heating at the microscale and resulting urban heat island (UHI) signatures [3,4]. The UHI effect in Toronto is uniquely influenced by the city's proximity to Lake Ontario where the temperature and humidity can be dictated by the lake and land breeze mesoscale phenomena [5]. As a northern city, residents are less adapted to extreme heat, and thus experience a lower temperature threshold concerning heat mortality or morbidity responses [6,7]. The heterogeneous nature of the built environment and resulting thermal impacts at various scales can have a compelling effect (both negative and positive) on the health of its residents. Urban heat-health research regularly operates at coarse scales and uses scattered environmental observations, while urban built features generally impact human health at fine scales [8,9]. The use of coarser scale environmental information has resulted in a deficiency in spatially congruent evidence linking urban form and human comfort. Locations containing natural surfaces (vegetation, water, etc.) and shade are routinely associated with reductions in summertime temperatures and improvements in thermal comfort (TC) [10,11]. Studies performed in Toronto demonstrate 'urban cool islands' [12], as well as associations between canopy cover and emergency response calls [13].

Although studies of heat-related morbidity and mortality have focused primarily on air temperature (T_a), TC is largely affected by microclimatic variations in solar and terrestrial radiation, relative humidity (RH), and wind speed (V_w) [14,15]. The mean radiant temperature (T_{mrt})—the combination of all short and longwave radiant fluxes experienced by a human [16]—is a significant variable to consider in outdoor TC research. Radiant heat gains are often the most significant contributor to thermal discomfort in warm conditions [17–20]. Hence, many models account for numerous weather variables, whether simple temperature–humidity indices or the commonly employed wet bulb globe temperature (WBGT) index used in sports, workplaces, and military [21,22], or the more complex rational energy budget that account for personal factors [23]. The various indices developed for use for outdoor exposures can be found elsewhere [24,25].

1.3. Mass Gatherings and Thermal Comfort

Mass gatherings are generally defined as a large number of people (ranging from 1000 to >25,000) at a specific location, for a specific purpose, and for a defined time frame [26]. Attendees of mass gatherings face unique health risks because these events create challenging environments for emergency medical services (EMS) response. High crowd density often limits spectator access to airflow, shade, and water, and the thermal insulation of surrounding bodies and metabolic heat generation adds to the heat load already induced by the thermal environment [27,28]. Heat-related illnesses are a leading cause of mortality at mass gatherings (leading with stampedes) [29], with game-time heat and humidity being a significant predictor of medical care needs [26], as are event type and other extreme weather [30,31].

The interface between climate and tourism is multifaceted and complex [32], and hence during international events, there is a higher likelihood of thermal discomfort and heat stress in spectators and even athletes, whether due to inexperience or maladaptation. Spectators and volunteers often account for the majority of emergency response or First Aid calls at large-scale sporting events (e.g., Atlanta

Olympics [33]), many of whom come from distant locations and are often poorly acclimatized to the local climate [34]. Contrarily, athletes often participate in heat acclimation training well in advance of distant competitions to prepare for competition in the local weather conditions where the competition is being held. They further possess a higher fitness level [35,36] and are more prepared for their activity, thus allowing the athletes to handle higher heat loads more efficiently. Furthermore, their motivation and their expectation of a warmer environment due to physical activity may also decrease their perceived thermal discomfort [37–40].

The current study utilizes a 53-station mesoscale monitoring network (mesonet) deployed for the PA15 Games across the GTA to gain strategic insight into: (1) temperature variability across the GTA during the summer of 2015, including the PA15 Games period; and (2) provide a case study analysis of the thermal conditions and perceptions connected to health at a hot, crowded venue during major PA15 Games events to demonstrate the value of site-specific weather stations. The project builds on the greater PA15 Games initiatives set to harness the related challenges of providing urban-scale weather, AQ, and health alerts and services during a major event [2].

2. Experiments

2.1. Study Site

Toronto, Canada (43.7182° N, 79.3774° W), the capital city of the Province of Ontario, is a dynamic metropolis along Lake Ontario's northwestern shore. It is the largest city in Canada, hosting over six million residents within the GTA. The city experiences a semi-continental climate, with a generally warm, humid summer and a cold, dry winter, modified by its location on the shores of Lake Ontario [41]. The three hottest months are June, July, and August, with average daily high temperatures of 23.8 °C, 26.6 °C, and 25.5 °C respectively. Located in the warmest climate zone in Canada, Toronto has experienced above average maximum temperature (T_{max}) in five of the seven summers between 2010 and 2016 [42] and is predicted to have doubled heat-related mortality by 2050 and tripled heat-related mortality by 2080 [43]. Heat-health alert and response systems have become the norm in such cities of dense occupation. The province of Ontario's new health evidence-based heat warning information system (HWIS) was designed to have an early notification service for public health decision-makers and community partners when health-threatening weather conditions are imminent. The HWIS, therefore, is better able to support the mobilization and communication of local resources to encourage targeted response actions to help protect people from health risks associated with extreme heat events [2]. The HWIS was used in Toronto for the 2015 summer season and the PA15 Games in attempt to minimize human heat-related morbidity during an influx of athletes and public spectators as a result of the PA15 Games.

2.2. Data Collection

ECCC completed the installation of a 53-station mesonet throughout the PA15 Games area (see Supplementary Material Figure S1). Of those 53 stations, 10 are permanent stations and 43 are compact stations that were temporarily installed. Figure 1 shows the general design of the compact weather stations. Each station was equipped with a black globe temperature sensor (Campbell Scientific, Inc., Logan, UT, USA) to record globe temperature (T_g) (°C), and either a Vaisala WXT520, Lufft WS601, or Lufft WS600 weather transmitter to record wind speed (ms^{-1}) and wind direction, T_a (°C), dewpoint temperature (T_d) (°C), and RH (%). Instrument height for all stations was 2.5 m above their respective surface. Data were collected at 1-min intervals using either a CR-1000 or CR-3000 Campbell Scientific datalogger. Forty-eight of the stations had $\leq 1.1\%$ of data missing, three stations had $< 8\%$ of data missing, and two stations had $< 18\%$ of data missing. A list of each station's name, local climate zone (LCZ), latitude, longitude, and further description, as well as station LCZ examples, can be found in the Supplemental Material (Table S1, Figure S2) based on LCZs classification from Stewart and

Oke [44]. Full raw mesonet data are available on the Government of Canada's Open Government Portal [45].

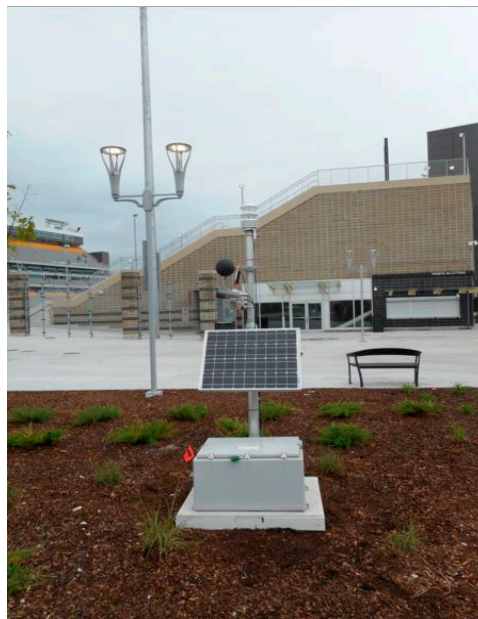


Figure 1. Hamilton Soccer Center mesonet station used to monitor environmental conditions during the PA15 Games' soccer events. Source: Environment and Climate Change Canada.

2.3. Heat Metric Calculation

From the meteorological variables collected by the mesonet, three heat metrics were calculated: the humidex, the WBGT index, and the COMFA human energy budget (EB) model. The COMFA EB model was used for the specific case study analysis during an anomalous heat event (Section 2.4). The maximum and minimum T_a values were additionally extracted. All were calculated based on the average observations of the previous hour.

Canadian meteorologists use the humidex to communicate an estimate of a perceived temperature—or one that the average human body would feel, given the combination of the T_a and RH of the air—as follows:

$$\text{Humidex} = T_a + 0.5555 \left[6.11e^{5417.7530 \left(\frac{1}{273.16} - \frac{1}{T_d} \right)} - 10 \right] \quad (1)$$

where T_a is the air temperature in °C and T_d is the dewpoint temperature in Kelvin.

The WBGT index was created in the early 1950s to limit serious heat illness outbreaks in the United States Armed Services training camps, and is commonly used in heat stress research [46]. The index is a weighted average of air temperature (T_a), the natural wet-bulb temperature (T_{nwb}), and globe temperature (T_g), calculated as:

$$\text{WBGT} = 0.7T_{nwb} + 0.2T_g + 0.1T_a \quad (2)$$

The WBGT index remains a convenient and comprehensive index of heat stress to monitor environmental conditions during manual labor and exercise in direct sunlight. Multiple sporting organizations, such as the Women's Tennis Association (WTA), the National Collegiate Athletic Association (NCAA), the International Federation of Association Football (FIFA), etc. use the WBGT index to protect both athletes and spectators during sporting events. Specific guidelines have been established by the American College of Sports Medicine (ACSM) for activity modifications to avoid experiencing heat stress (e.g., rest breaks, water consumption, limited uniform attire) [47]. Risk of

exertional heat illness begins for fit and acclimatized competitors at a WBGT of 22.3 °C with the need to monitor fluid intake. According to the ACSM, WBGTs above 30.1 °C would limit the amount of activity or add breaks. The PA15 Games threshold for soccer games utilized a 32 °C threshold set by FIFA to impose mandatory cooling breaks.

2.4. Thermal Comfort Case Study

A focused case study is provided for the Hamilton Soccer Center due to: (1) the venue's diagnosis as a high-heat-exposure area during the months the PA15 Games took place (Section 3.1); and (2) the multiple complaints received from spectators, volunteers, and on-site paramedics alike regarding weather conditions at the venue during PA15 Games events (Section 3.3). For the case study, the human EB values for spectators and athletes were calculated to determine the thermal discomfort experienced by the spectators based on the minutely weather data from the nearby mesonet station at the soccer stadium (Figure 1).

The COMFA human EB model is a mathematical model designed to estimate the TC of an individual at a given place and time. Studies have both tested and incorporated revisions into the model to ensure agreement between predicted TC estimates and actual TC responses during both sedentary and non-sedentary activity [13,48–50]. The model requires meteorological inputs (T_a , absorbed radiation (R_{abs}), RH, and V_w) and personal inputs (metabolic activity, M_{act} , and activity velocity, V_a) to produce a human EB in Wm^{-2} , based on the following summation:

$$B = M + R_{abs} - E - C - L_{emit} \quad (3)$$

where M is the metabolic heat generated by a human, R_{abs} is the absorbed radiation, E and C are the total evaporative and convective heat losses, respectively, and L_{emit} is longwave radiation emitted from a human. All fluxes are in Wm^{-2} . Table 1 displays the subjective interpretation of the model output values for sedentary individuals. We present details specific to the current study below, while the full model can be found elsewhere [49–51].

2.4.1. Absorbed Radiation

The R_{abs} was estimated from the T_g , first by calculating the T_{mrt} (Equation (4)) [16] and converting to R_{abs} in Wm^{-2} (Equation (5)).

$$T_{mrt} = \left[(T_g + 273.15)^4 + \frac{(1.10 \times 10^8) V_w^{0.71}}{\varepsilon(D^{0.4})} (T_g - T_a) \right]^{\frac{1}{4}} - 273.15 \quad (4)$$

where T_a is air temperature in °C, T_g is globe temperature in °C, V_w is wind speed in ms^{-1} , ε is the globe emissivity (0.95), and D is the globe diameter (0.150 m).

$$R_{abs} = \sigma(T_{mrt} + 273.15)^4 \quad (5)$$

where σ is the Stefan–Boltzmann constant ($5.67 \times 10^{-8} \text{Wm}^{-2}\text{K}^{-4}$). However, T_g values are based on a black spherical human with an albedo near 0, yet humans are mainly cylindrical-shaped with an average albedo of about 0.37 [48,52]; therefore, the R_{abs} values calculated from the black globe in Equation (5) would overestimate the actual R_{abs} experienced by a human, mainly due to the black matte color. Hence, a correction factor was applied to each R_{abs} value to account for color differences and geometric differences by sun angle between a cylinder and globe, as in Grundstein et al. [51]. An effective area of 0.78 was applied for a standing human [53]. All physiological input values for the athletes and spectators are shown in Table 2 and outlined below.

Table 1. Subjective interpretation of the COMFA human energy budget model output values for a non-active and active individual [48,50,54].

Subjective Interpretation Non-Active	Model Output (Wm ⁻²)	Subjective Interpretation Active	Model Output (Wm ⁻²)
‘Cold’ (−2)	−200 to −121		
‘Slightly Cool’ (−1)	−120 to −51	‘Cool’ (−1)	−120 to −20
‘Neutral’ (0)	−50 to +50		
‘Slightly Warm’ (+1)	+51 to +120	‘Neutral’ (0)	−20 to +150
‘Warm’ (+2)	+121 to +200	‘Warm’ (+1)	+151 to +250
‘Hot’ (+3)	≥ +201	‘Hot’ (+2)	≥ +251

Table 2. Personal inputs used for the spectator and athlete (soccer player) in the COMFA model.

	Variable	Value
Spectator	M_{act}	166 Wm ⁻²
	V_a	0.2 ms ⁻¹
	clo	0.33
	A_{eff}	0.78
	α	0.37
Athlete	M_{act}	varying
	V_a	varying
	clo	0.37
	A_{eff}	0.78
	α	0.37

2.4.2. Metabolic Intensity

Spectator physiological inputs were modeled as a constant “very excited, emotional, and cheering” individual (metabolic equivalents (MET) = 3.0) [55] (see Table 2). As compared to spectators, the metabolic rate of athletes is much higher and more variable. Estimating TC is thus considerably more challenging, yet still valuable due to the running-stopping nature of the game. Information regarding the athletes’ metabolic intensities were not collected at the PA15 Games. Hence, rather than using a constant (and thus largely inaccurate) metabolic intensity of 8.0 METs from the compendium of physical activities [55]), we applied heart rate (HR) and V_a data from a competitive women’s soccer game completed at Texas Tech University in Spring 2017 from a midfielder as an analogue (data were from Polar Team Pro HR monitors, providing HR and V_a in 1 s intervals, averaged to 1 min). The HR estimates collected in Texas are assumed to be similar to those experienced by a soccer player at the PA15 Games and provide a much more realistic estimate of average metabolic intensities of soccer players in normal game situations. Analogous to the energy expenditure estimation methods [56,57], inputs of age (25 years of age), average resting HR, activity HR, and gender were used to estimate the energy expenditure of a female or male midfielder, and output in METs (1 MET = 58.15 Wm⁻²).

2.4.3. Clothing

Estimates of clothing ensemble insulation were determined by:

$$I_{cl} = 0.161 + 0.835 \sum I_{clu} \tag{6}$$

where I_{clu} is the effective thermal insulation of the individual garments. Spectator clothing estimations were based on typical summertime attire, which includes underwear, a T-shirt, shorts, light socks, and sandals (0.33 clo) [58]. Athletic soccer clothing estimations were based on the standard configuration of a soccer uniform (i.e., briefs/panties, shirt, shorts, knee-length thick socks, and athletic shoes (0.37 clo)).

The EB experienced by spectators and athletes was determined by using the subjective interpretation shown in Table 1. The scales differ for active and non-active individuals because those performing physical activity are prepared, accepting, and expectant of slightly uncomfortable conditions, entitled the activity skewing effect [12,50].

2.5. Informal and Formal Evidence of Heat Stress

Insights concerning thermal discomfort and heat stress were also obtained through reports from the ECCC, Hamilton Paramedic Service, St. John Ambulance, and Twitter feed within the stadium. First Aid and EMS data were provided by the paramedic agencies working at the soccer venue as recorded during each event of interest.

Social media, particularly Twitter, has become a rising data source for social research, allowing for a better understanding of complex human behaviors [59,60], social dynamics [61,62], emergence management and risk assessment [63–66], and has specifically demonstrated usefulness for assessing weather and extreme heat impacts [67,68]. Twitter feed was collected using the Twitter Streaming Application Program Interface (API) [69]. The Twitter feeds were filtered for the area in and closely surrounding the Hamilton Soccer Center (geographic extent: [43.259537, −79.834990; 43.259537, −79.816160; 43.242543, −79.819363; 43.248090, −79.840234]) to assess the spectator perception of heat at the event, and were focused on 25 and 26 July 2015 when the men’s bronze medal soccer match, women’s gold medal soccer match, and men’s gold medal soccer match took place.

3. Results

3.1. Urban Heat Variability across the PA15 Games Area

The station-specific seasonal summer averages for each heat stress metric (T_{max} , maximum humidex, and maximum WBGT index) are presented by size and color of circles in Figure 2. The stations with the highest T_{max} values are concentrated near downtown Toronto and Hamilton, two of the most built-up and populated urban areas within the PA15 Games region. It is evident that the area between Lake Erie and Lake Ontario creates a very humid environment as high humidex and WBGT index values (both highly sensitive to the amount of moisture in the air) are observed at stations located between the two lakes. Thus, the downtown area, with less vegetation and moisture, presents comparatively lower humidex and WBGT index values, yet higher T_{max} values due to more radiant absorption in the built-up urban area. Overall, however, the T_{max} , humidex, and WBGT index metrics’ values vary minimally among the stations, with ranges of <4 °C for all.

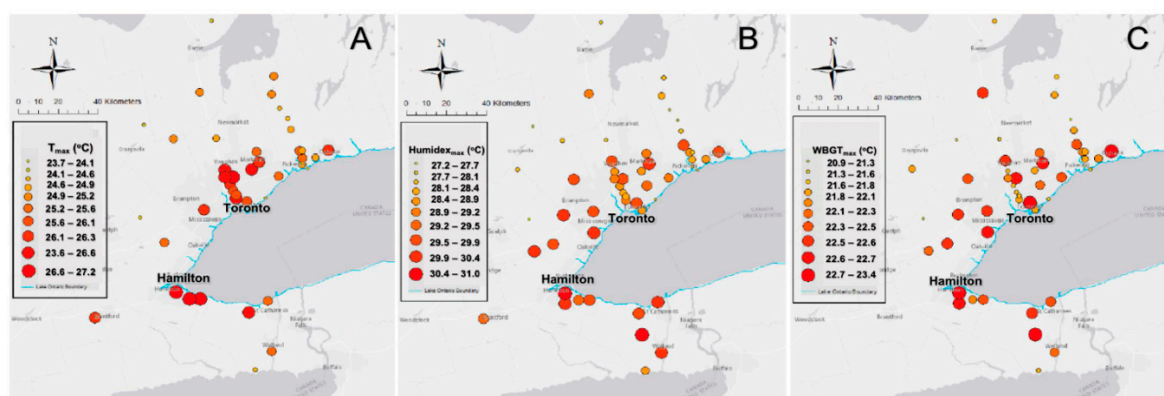


Figure 2. Station-specific seasonal summer maximum (A) air temperature, (B) humidex, and (C) WBGT index averages. Each circle represents an individual station. The color and size of the circle reflect the magnitude of the heat metric, with darker and larger circles indicating higher values. Note that the scales differ between plots.

Much of the heat metric variability mapping findings are devoted to detecting areas/venues with heightened heat exposure during the summer months, known as ‘hot spots’. Within the GTA, the city of Hamilton emerges as a hot spot across all heat metrics, with the Hamilton Soccer Center station ranking within the top 4% of the T_{max} , humidex, and WBGT index metric seasonal summer average values among all of the 53 stations. A two-sample t-test confirmed that the Hamilton Soccer Center station was significantly different from the mean of all stations for the T_{max} , humidex, and WBGT index heat metrics. For these reasons, athlete and spectator energy budgets were modeled at three PA15 Games soccer events in late July at the Hamilton Soccer Center to assess the extent to which the weather conditions in Hamilton had an impact on human TC.

3.2. Stadium Thermal Comfort

Figure 3a displays the temporal changes of the spectator energy budgets modeled for the duration of the game and the preceding and succeeding hour (warm-up and medal ceremony). The EB analysis showed TC to fall between the range of ‘slightly cool’ (no threat of heat stress) to ‘hot’ (dangerous threat of heat stress). The average EB value was 90.3 Wm^{-2} for the men’s bronze medal match, 249.6 Wm^{-2} for the women’s gold medal match, and 67.1 Wm^{-2} for the men’s gold medal match (Figure 4). Even with low metabolic rate modeling ($M_{act} = 166 \text{ Wm}^{-2}$), the spectator thermal comfort reached well above the ‘warm’ zone ($> 121 \text{ Wm}^{-2}$) (potential for heat stress), and commonly remained in the ‘slightly warm’ range (moderate threat of heat stress) or higher for the second half of each soccer event. Overall, a steady increase in the estimated energy budgets throughout the game period is observed for all three matches (Figure 3a). For average hourly meteorological data at Hamilton Soccer Center on the days the soccer matches took place, please see Supplementary Material Table S2.

Peak EB values, and therefore the greatest thermal discomfort, occurred during the women’s gold medal soccer match, where spectators remained in the ‘hot’ range for the majority of the event (162 min) (Figure 3a). The men’s bronze medal match recorded a dangerous threat of heat stress for 27 min total. The most thermally comfortable event was the men’s gold medal match, which only exceeded the ‘hot’ threshold for 12 min.

Each EB component by match is displayed in Figure 4, demonstrating the important influence of R_{abs} in increasing the heat load, with critical heat losses arising from evaporation and convection. These heat losses vary minimally as the metabolic rates and movement were constant in the model, thus any variability of evaporation is due to changing wind and activity speeds and RH, while convection is primarily controlled by the T_a . In the women’s gold medal game, a much higher T_a and RH with low V_w resulted in a lower ability to lose heat and thus a higher overall EB and risk of heat stress.

The modeled athlete energy budgets assumed that the athletes remained outdoors for the duration of the game, the half time break, and the preceding hour (warm-up). Figure 3b displays the temporal changes of the modeled athlete (midfielder) energy budgets for the three matches. During the women’s gold medal match, the athletes endured ‘hot’ budget levels for almost the entire event (97 min total), whereas the men’s bronze and gold medal matches reported a dangerous threat of heat stress during the second half of the game for 16 and 18 min total, respectively. Figure 4 demonstrates the large variability in the metabolic rates, evaporation, and convection as compared to the spectators. The differences in evaporative and convective heat losses between athletes and spectators are primarily due to a higher metabolic rate of athletes (causing a higher sweating rate and thus evaporation of sweat) and activity speed, respectively.

The dip in player EB values between the start and end of each soccer match can be attributed to the approximately 20-min half-time break when players generally sit and a decrease in M_{act} occurs. The energy flux gains and losses that produce the final athlete energy budget (based on Equation (3)) for each of the three events are shown in Figure 4. The EB follows a pattern strongly related to M_{act} for the men’s bronze and gold medal matches, and to R_{abs} for the women’s gold medal match. These results are primarily due to a larger variance in V_w during the women’s gold medal match, which causes R_{abs} to vary more due to the method of calculating T_{mrt} (based on Equation (5)).

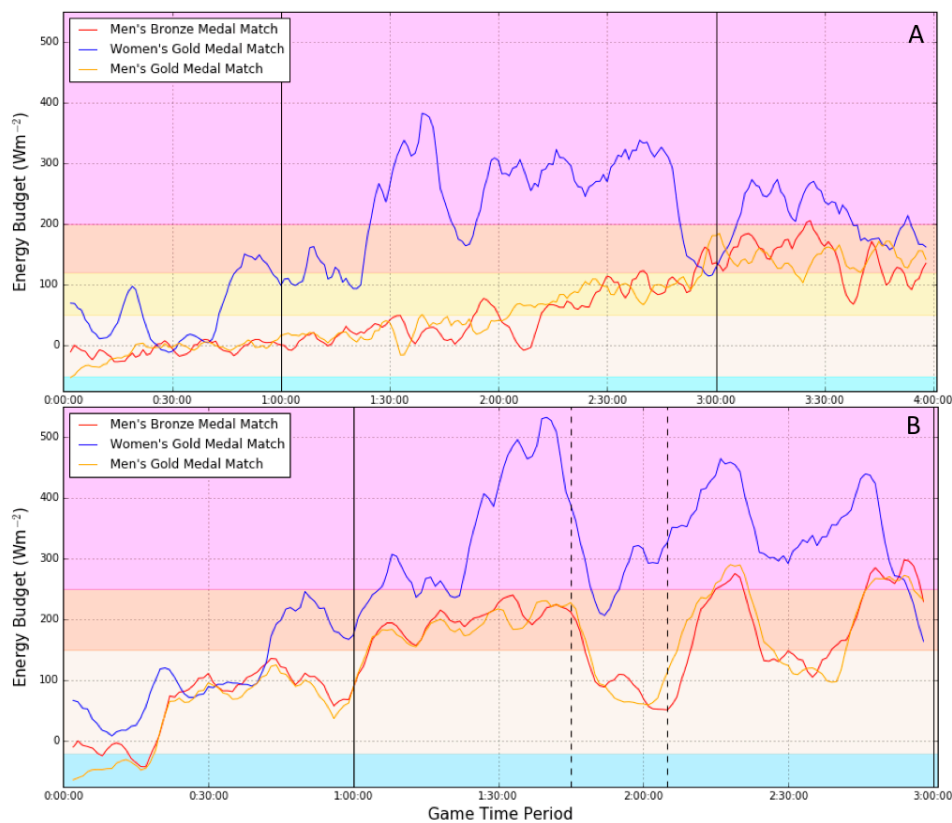


Figure 3. Temporal changes of the modeled energy budget of the spectators (A) and athletes (midfielders) (B). Lines represent three games: red line–Men’s Bronze Medal Match, 13:05–15:05, 25 July 2015; blue line–Women’s Gold Medal Match, 18:35–20:35, 25 July 2015; yellow line–Men’s Gold Medal Match, 13:05–15:05, 26 July 2015. Game start and end times are indicated by vertical solid lines. In (B), the half-time break beginning and end times are also designated by vertical dashed lines. The background colors are indicative of the non-active spectator (A) and athlete performing physical activity (B) subjective interpretation to the COMFA EB model output.

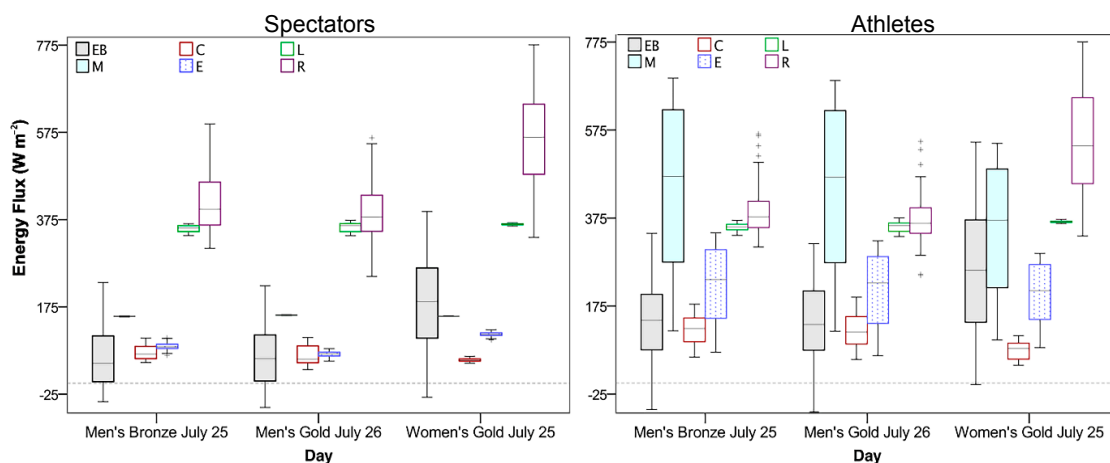


Figure 4. Stem and leaf box plot depicting the estimate range of the energy budget values (EB) on each day (spectators left plot; athletes right plot). Energy flux gains and losses also shown: metabolic heat gain (M); absorbed radiation heat gain (R_{abs}); convective heat loss (C); evaporative heat loss (E); and longwave emission heat loss (L_{emit}) in Wm^{-2} . The interquartile range (IQR) is indicated by the length of each box plot (25th to 75th percentiles), with outliers (values 1.5–3 IQRs from box end) marked by \circ .

3.3. Spectator and EMS Response

Anecdotal evidence from Twitter, ECCC reports, Hamilton Paramedic Service, and St. John Ambulance revealed that a combined 10 heat-related EMS calls were made during the men's bronze medal and women's gold medal soccer matches on 25 July, and that 13 heat-related EMS calls were made during the men's gold medal soccer match on 26 July. All heat-related EMS calls were made directly from the Hamilton Soccer Center venue. However, as the majority of heat-related EMS calls were made during the men's gold medal match, these results emphasize that mass gatherings have the ability to increase heat stress and thus the number of heat-related illnesses occurring at lower EB levels, and that more attendees were likely present at the men's gold medal match.

According to ECCC, a spectator that attended the men's bronze medal soccer match stated that "on the way there [the stadium], there were long lines for the shuttle buses, and several people had to be treated for heat stroke" (D. Sills (ECCC), personal communication, 2017). Similarly, on 26 July on-site paramedics noted that the conditions at the venue were "very hot" and that they "had to call in crews to stand-by in hard enclosure [the stadium] due to the call volume" (Hamilton Paramedic Service, personal communication, 3 February 2017). Such anecdotal information is vital in planning future large-scale sporting events.

A total of 150 Tweets were obtained from the area during the soccer events, with eight complaining of the heat. These Tweets mentioning heat conditions, from personnel inside/around the Hamilton Soccer Center, on the days that the three soccer matches took place are listed below.

- "The sun is burning!"
- "The very long lineup for water at #URU vs #MEX. Many more water stations needed."
- "Enjoying the hot day watching the gold medal men's #soccer"
- "Half time. Holy cow, it's hot out here. Can't imagine what it's like on the turf."
- "Today the heat is unbearable in Hamilton. Already several players of both teams look exhausted!!!" (Translated from Spanish)
- "With this heat, the black color of the shirt does not help!!!" (Translated from Spanish)
- "It is very hot" (Translated from Spanish)
- "Embracing the heat with a stroll under the trees at Gage Park"

The perceived heat-related EMS calls and anecdotal communication mentioned above are consistent with the TC results from the modeled spectator energy budgets during each of the three soccer events. However, we cannot complete a spatial quantification of spectator TC because spectator energy budgets were modeled based on weather data at only one location at the Hamilton Soccer Center (see Figure 1). Further, the exact locations of where the heat-related Tweets and EMS calls were made within the stadium are unknown.

4. Discussion

4.1. Geospatial Station Summertime Averages

Across the GTA, between-station summertime average values showed low variability for T_{max} , humidex and the WBGT, yet some influence from vegetation, water sources, and/or built-up areas are present. The overall small spatial heterogeneity, however, indicates good mixing from wind and that differences in the LCZ and surface cover among stations had little effect on heat metric values. Since Toronto experienced below average temperatures during the summer of 2015 [42], few heat waves were present and hence a lower UHI intensity could build. Furthermore, the maps presented examine averages of all days (two months) rather than during distinct days or events, which provides more robust estimates and smooths intra-urban and seasonal variability. However, the geospatial map results highlight that warmer temperatures and higher humidity are present in both the downtown Toronto area and the Hamilton area. Oke and Hannell [70] have shown that the local steelworks

in Hamilton is responsible for producing its own UHI. Similarly, Blair [71] found that within the Toronto–Hamilton urban airshed, two large UHIs are present in the downtown areas of Toronto and Hamilton. The presence of the Great Lakes also enhances the humidity, yet we did not differentiate days by wind direction and speed, and thus cannot determine the extent to which the heat metric values were affected by the lake moisture, breeze, and/or circulation.

Spatial maps are helpful to guide urban planners looking to limit the highest heat levels in a city, and also help First Aid and emergency responders in determining high-risk locations for heat stress [12,13,72]. Any newly planned large-scale sporting events in the GTA can also make use of this new information for organization purposes, especially given that the mesonet station locations were situated at or near venues. Finally, such maps may inform city public health officials of the locations of increased heat, radiation, and humidity exposure at a finer intra-urban scale during the summer season [73,74]. Particular example applications of these mesonet geospatial maps are the prioritization of hot spot locations for the delay of electricity shut-offs by energy policy managers [75], examining heat or cold exposure during non-motorized transit [76] that occurs often when traveling to and from sporting events, and venue improvements.

Other urban heat variability studies have utilized similar mesonets across cities (e.g., Oklahoma City [77]; Boston, New York, Philadelphia, Baltimore mesonets [78]) to demonstrate fundamental spatiotemporal variations in intra-urban heat variability, information which aids in precipitation and storm predictions (as completed for the PA15 Games in Toronto [2]), as well energy efficiency, public safety, security, transportation and many other critical functions in society [79]. Without the mesonet station on site, spectator and athlete thermal comfort analysis would not have been possible. No other study has yet to apply energy budget modeling to spectators at a sporting event, however, such a method may become more important at large-scale sporting events in hot–humid climates in the coming years, such as the 2020 Summer Olympics in Tokyo, Japan (e.g., [80]) and the 2022 FIFA World Cup in Qatar.

4.2. Heat Stress at Sports Events

During hot weather, many individual characteristics influence who will be affected by heat, either for physiological or behavioral reasons [81]. Athletes, attendees at mass gatherings, and tourists are specific population subsets that can be negatively affected during episodes of hot weather because they are more likely to be outdoors, in large crowds, and/or exerting themselves. The anecdotal evidence from spectators, ECCC employees, and paramedics alike regarding the thermal discomfort experienced during the soccer events that took place on 25 and 26 July demonstrates that EMS personnel may have been unprepared to handle the unanticipated influx of heat-related illness complaints recorded at the Hamilton Soccer Center. With both spectator and athlete thermal comfort exceeding the ‘hot’ subjective interpretation threshold for all three events, venue design modifications (which can partially control and attenuate undesirable environmental conditions to improve TC, decreasing the chance of heat illnesses [82,83]) should be considered for the soccer stadium and other outdoor facilities that intend to hold mass gatherings in Hamilton.

Reducing the R_{abs} by a human by increasing shade and implementing natural surfaces will have a positive effect on human TC and heat health and will reduce summer temperatures [10,72,84]. Venue modifications could include field-surface-type transition from synthetic turf to natural grass, as the radiational properties of such surfaces affects both the T_a and the interactions of total radiation fluxes with the human body within a microclimate [85], and/or the addition of fans to improve ventilation and shade sails over the stadium seats based on orientation and sun angle [86]. Such modifications could greatly impact short-term TC during sporting events since the energy flux gains and losses show that the final energy budget values are strongly influenced by a combination of the R_{abs} and M_{act} . A study by Bouyer et al. [87] also found that solar radiation and wind speeds were important factors in TC within stadiums, specifically on the perimeter of athletic fields. Further TC studies concur that radiation is an important variable to consider in outdoor TC research since

radiation (T_{mrt} or R_{abs}) is commonly the largest contributor to the human energy budget equation and has a strong negative relationship with human TC [15]. However, often radiation or a proxy for radiant heat (such as the globe temperature) is not measured at traditional weather stations.

The sensitivity of the both human energy balance and heat-related morbidity/mortality to T_{mrt} or R_{abs} variations warrants greater focus on new installations of radiant heat sensors, pyranometers, and/or improved assessment of city sky view factors (e.g., [80,88]) to improve spatial modeling of hot spots, which can serve as a guide to EMS deployment resources, energy use, and city planning efforts. Positioning EMS resources in such hot spots during heat waves and/or large-scale events, and providing sufficient staffing, is a vital strategy for reducing heat-related illness cases [89].

The athletes endured the highest EB rates overall leading to recommendations to maximize athlete safety and performance and establish on-site emergency response plans [35,90], particularly for athletic venues located in areas with enhanced heat [34,91,92]. Yet often times, mass gatherings and the large spectator volumes can lead to potentially higher patient volumes. This increase in spectator heat-illness versus athletes at higher metabolic loads may stem from the idea that poor health and fitness are dominant risk factors leading to heat stress [93]. Exercise induces physiological adaptations that improve thermoregulation, attenuate physiological strain, reduce the risk of serious heat illness, and improve aerobic performance in warm-hot environments [94]. Therefore, integrating physical activity into daily life routines to improve cardiovascular health is a viable preventative and sustainable heat stress adaptation strategy for individuals, whereas other recognized risk factors such as age and urbanization have limited adaptation potential [93]. Therefore, considering the inter-individual differences of humans (specifically anthropometry, fitness, gender, and acclimatization status) in addition to the thermal environment can improve the prediction of heat stress [95].

4.3. Limitations and Future Recommendations

Although select mesonet stations assembled by the Meteorological Service of Canada (MSC) of ECCC in preparation for the PA15 Games began collecting data in May 2015, the full array of stations was not completely operational until the beginning of July 2015. Additionally, the gradual de-commission of the stations began in September 2015. As a result, the meteorological dataset used to accomplish the objectives of this study was limited to only two months of data (July and August 2015) in order to incorporate data from all 53 stations. Knowing this, ECCC should consider the permanent operational reinstatement of a mesonet designed to construct a real-time evidence base for analysis that may be used to determine cutting-edge heat-health relationships in Toronto in the future. Additionally, the windspeed applied for in-stadium TC estimations was that collected by the mesonet station placed in open air just outside Hamilton Soccer Center (see Figure 1), however wind speeds in the semi-outdoor environment of the stadium and in the crowd are slower [87], and thus thermal discomfort was likely underestimated. Finally, given that numerous attendees were from out of the country, they may have been unable to use their cell-phones to access social media, and thus the Twitter-related analysis may also be an underestimate.

5. Conclusions

Novel fine-scale meteorological data from a within-city 53-station mesonet was used to calculate numerous hourly heat metric values for various locations across the GTA for July and August 2015. This unique dataset was applied in two ways: (1) to determine the GTA's areas of escalated heat exposure; and (2) to showcase the benefits of using outdoor human energy budget modeling as a meaningful tool for thermal comfort and heat stress assessment at mass gathering events. Results reveal intra-urban variation in heat exposure dependent on heat metric used (i.e., WBGT versus air temperature). The downtown Toronto corridor displayed higher heat levels based on maximum air temperature, yet the humidex and WBGT metrics showed lower heat levels in the downtown due to less humidity. The overall consensus among all heat metrics showed that Hamilton, Ontario maintained the highest levels of heat throughout the summer of 2015 and is an area of escalated

risk for heat-related illness. Spectator and physically active athlete energy budgets at the Hamilton Soccer Center during PA15 soccer matches were significantly influenced by absorbed radiation by a human and metabolic activity, values which are not included in most heat stress metrics such as the humidex or heat index.

Results emphasize the various potential benefits and products (e.g., heat vulnerability maps, public real-time local weather information) that arise from implementing localized mesonet stations for public health protection. The ability to obtain highly resolved data at urban locations that are both built-up and highly visited by large crowds further enhances the impact and utility of said environmental information for planning, design, and health. Future large-scale sporting events will benefit from the mesonet and human thermal comfort information for resource deployment (e.g., EMS personnel) and for event planning purposes.

Supplementary Materials: The following are available online at <http://www.mdpi.com/2073-4433/9/8/321/s1>. Table S1: Mesonet weather station locations, LCZs, and surface covers. Considering the surrounding environment (up to 250 m), the LCZ of a station was determined post-site selection process using notes and photos taken by the MSC while on-site and Google Earth. Any LCZ or height differences among the stations were accounted for upon installation. The compact stations were primarily installed in 2014 and decommissioned in Fall 2015 and were operational from May 2015 through September 2015. However, this study focuses only on the data collected during July and August; the months during which the PA15 Games took place. Table S2: Hamilton Soccer Center station average hourly meteorological data for 25–26 July 2015. Figure S1: Mesonet monitoring network stations (black circles) dispersed across the Games area. The stations are generally located near the Games venues. Figure S2: Urban and rural mesonet weather station LCZ examples. Figure S3: Energy budget and energy flux components (MET—metabolic activity; CONV—convective heat loss; EVAP—evaporative heat loss; R_{net} —net difference between absorbed radiation and emitted radiation by the body) for each game. Vertical lines indicate start and stop time with halftime centered between lines. Figure S4: Energy budget and energy flux components (MET—metabolic activity; CONV—convective heat loss; EVAP—evaporative heat loss; R_{net} —net difference between absorbed radiation and emitted radiation by the body) for each game. Vertical lines indicate start and stop time with halftime centered between lines. MET is constant at 150 W m^{-2} for spectators. Note scale change in Women's Gold Medal match.

Author Contributions: A.J.H. and J.K.V. conceived and designed the experiments; D.H. and M.M. provided data and guidance from Environment and Climate Change Canada for data usage and analysis; A.J.H., I.S.-F. and J.K.V. performed the analysis; R.D.B. and G.C. advised methodology; A.J.H. wrote the paper while all authors provided text portions and constructively reviewed the paper.

Funding: The mesonet system and its support was funded by the Government of Canada.

Acknowledgments: The authors are grateful to Environment and Climate Change Canada, Hamilton Paramedic Service, and St. John Ambulance for providing us with mesonet monitoring network meteorological data and anecdotal emergency medical service data, respectively. A.J. Herdt was partially funded on an NSF EAPSI award during the completion of this work. Authors would like to acknowledge Texas Tech University for supporting A.J. Herdt's completion of the current study. Special thanks are also given to Marc Lochbaum and the TTU women's soccer team for collecting heat-related data to use as more accurate estimates of metabolic experienced during a typical warm weather soccer game.

Conflicts of Interest: The authors declare no conflict of interest.

References

1. Eichner, E.R. SSE #86: Heat Stroke in Sports: Causes, Prevention and Treatment. *Sports Sci. Exchtr.* **2002**, *15*, 86.
2. Joe, P.; Belair, S.; Bernier, N.B.; Bouchet, V.; Brook, J.R.; Brunet, D.; Burrows, W.; Charland, J.P.; Dehghan, A.; Driedger, N. The Environment Canada Pan and ParaPan American Science Showcase Project. *Bull. Am. Meteorol. Soc.* **2017**. [[CrossRef](#)]
3. Rinner, C.; Hussain, M. Toronto's urban heat island-exploring the relationship between land use and surface temperature. *Remote Sens.* **2011**, *3*, 1251–1265. [[CrossRef](#)]
4. Wang, Y.; Berardi, U.; Akbari, H. Comparing the effects of urban heat island mitigation strategies for Toronto, Canada. *Energy Build.* **2016**, *114*, 2–19. [[CrossRef](#)]
5. Mariani, Z.; Dehghan, A.; Joe, P.; Sills, D. Observations of Lake-Breeze Events During the Toronto 2015 Pan-American Games. *Bound.-Lay. Meteorol.* **2018**, *166*, 113–135. [[CrossRef](#)]

6. Hartz, D.A.; Brazel, A.J.; Golden, J.S. A comparative climate analysis of heat-related emergency 911 dispatches: Chicago, Illinois and Phoenix, Arizona USA 2003 to 2006. *Int. J. Biometeorol.* **2013**, *57*, 669–678. [[CrossRef](#)] [[PubMed](#)]
7. Sheridan, S.C.; Kalkstein, L.S. Progress in heat watch-warning system technology. *Bull. Am. Meteorol. Soc.* **2004**, *85*, 1931–1941. [[CrossRef](#)]
8. Jenerette, G.D.; Harlan, S.L.; Buyantuev, A.; Stefanov, W.L.; Declet-Barreto, J.; Ruddell, B.L.; Myint, S.W.; Kaplan, S.; Li, X. Micro-scale urban surface temperatures are related to land-cover features and residential heat related health impacts in Phoenix, AZ USA. *Landsc. Ecol.* **2016**, *31*, 745–760. [[CrossRef](#)]
9. Harlan, S.L.; Declet-Barreto, J.H.; Stefanov, W.L.; Petitti, D.B. Neighborhood effects on heat deaths: Social and environmental predictors of vulnerability in Maricopa County, Arizona. *Environ. Health Perspect.* **2013**, *121*, 197. [[PubMed](#)]
10. Giannakis, E.; Bruggeman, A.; Poulou, D.; Zoumides, C.; Eliades, M. Linear parks along urban rivers: Perceptions of thermal comfort and climate change adaptation in Cyprus. *Sustainability* **2016**, *8*, 1023. [[CrossRef](#)]
11. Brown, R.D.; Vanos, J.K.; Kenny, N.A.; Lenzholzer, S. Designing Urban Parks That Ameliorate the Effects of Climate Change. *Landsc. Urban Plan.* **2015**, *138*, 118–131. [[CrossRef](#)]
12. Vanos, J.K.; Warland, J.S.; Gillespie, T.J.; Slater, G.A.; Brown, R.D.; Kenny, N.A. Human energy budget modeling in urban parks in Toronto and applications to emergency heat stress preparedness. *J. Appl. Meteorol. Climatol.* **2012**, *51*. [[CrossRef](#)]
13. Graham, D.A.; Vanos, J.K.; Kenny, N.A.; Brown, R.D. The relationship between neighbourhood tree canopy cover and heat-related ambulance calls during extreme heat events in Toronto, Canada. *Urban For. Urban Green.* **2016**, *20*. [[CrossRef](#)]
14. Erell, E.; Pearlmutter, D.; Boneh, D. 236: Effect of high-albedo materials on pedestrian thermal comfort in urban canyons. *Simulation* **2012**, 8–11.
15. Middel, A.; Selover, N.; Hagen, B.; Chhetri, N. Impact of shade on outdoor thermal comfort—A seasonal field study in Tempe, Arizona. *Int. J. Biometeorol.* **2016**, *60*, 1849–1861. [[CrossRef](#)] [[PubMed](#)]
16. Thorsson, S.; Lindberg, F.; Eliasson, I.; Holmer, B. Different methods for estimating the mean radiant temperature in an outdoor urban setting. *Int. J. Clim.* **2007**, *27*, 1983–1993. [[CrossRef](#)]
17. Johansson, E.; Thorsson, S.; Emmanuel, R.; Krüger, E. Instruments and methods in outdoor thermal comfort studies—The need for standardization. *Urban Clim.* **2014**, *10*, 346–366. [[CrossRef](#)]
18. Kántor, N.; Lin, T.-P.; Matzarakis, A. Daytime relapse of the mean radiant temperature based on the six-directional method under unobstructed solar radiation. *Int. J. Biometeorol.* **2014**, *58*, 1615–1625. [[CrossRef](#)] [[PubMed](#)]
19. Taleghani, M.; Kleerekoper, L.; Tenpierik, M.; Van Den Dobbelsteen, A. Outdoor thermal comfort within five different urban forms in the Netherlands. *Build. Environ.* **2015**, *83*, 65–78. [[CrossRef](#)]
20. Hodder, S.G.; Parsons, K.C. The effects of solar radiation on thermal comfort. *Int. J. Biometeorol.* **2007**, *51*, 233–250. [[CrossRef](#)] [[PubMed](#)]
21. Lemke, B.; Kjellstrom, T. Calculating workplace WBGT from meteorological data: A tool for climate change assessment. *Ind. Health* **2012**, *50*, 267–278. [[CrossRef](#)] [[PubMed](#)]
22. ISO. *ISO 7243: Ergonomics of the Thermal Environment—Assessment of Heat Stress Using the WBGT (Wet Bulb Globe Temperature) Index*; International Organization for Standardization: Geneva, Switzerland, 2017.
23. Havenith, G.; Fiala, D. Thermal Indices and Thermophysiological Modeling for Heat Stress. *Compr. Physiol.* **2015**, *6*, 255–302. [[PubMed](#)]
24. Epstein, Y.; Moran, D.S. Thermal comfort and the heat stress indices. *Ind. Health* **2006**, *44*, 388–398. [[CrossRef](#)] [[PubMed](#)]
25. de Freitas, C.R.; Grigorieva, E.A. A comparison and appraisal of a comprehensive range of human thermal climate indices. *Int. J. Biometeorol.* **2017**, *61*, 487–512. [[CrossRef](#)] [[PubMed](#)]
26. Perron, A.D.; Brady, W.J.; Custalow, C.B.; Johnson, D.M. Association of heat index and patient volume at a mass gathering event. *Prehosp. Emerg. Care* **2005**, *9*, 49–52. [[CrossRef](#)] [[PubMed](#)]
27. Helbing, D.; Johansson, A. Pedestrian, Crowd, and Evacuation Dynamics. *Encycl. Complex. Syst. Sci.* **2013**, *16*, 6476–6495.
28. Stewart, I.D.; Kennedy, C.A. Metabolic heat production by human and animal populations in cities. *Int. J. Biometeorol.* **2017**, *61*, 1159–1171. [[CrossRef](#)] [[PubMed](#)]

29. Steffen, R.; Bouchama, A.; Johansson, A.; Dvorak, J.; Isla, N.; Smallwood, C.; Memish, Z.A. Non-communicable health risks during mass gatherings. *Lancet Infect. Dis.* **2012**, *12*, 142–149. [[CrossRef](#)]
30. Milsten, A.M.; Maguire, B.J.; Bissell, R.A.; Seaman, K.G. Mass-gathering medical care: A review of the literature. *Prehosp. Disaster Med.* **2002**, *17*, 151–162. [[CrossRef](#)] [[PubMed](#)]
31. Milsten, A.M.; Seaman, K.G.; Liu, P.; Bissell, R.A.; Maguire, B.J. Variables influencing medical usage rates, injury patterns, and levels of care for mass gatherings. *Prehosp. Disaster Med.* **2004**, *18*, 334–346. [[CrossRef](#)]
32. Scott, D.; Lemieux, C. Weather and climate information for tourism. *Procedia Environ. Sci.* **2010**, *1*, 146–183. [[CrossRef](#)]
33. Wetterhall, S.F.; Coulombier, D.M.; Herndon, J.M.; Zaza, S.; Cantwell, J.D. Medical care delivery at the 1996 Olympic Games. *J. Am. Med. Assoc.* **1998**, *279*, 1463–1468. [[CrossRef](#)]
34. Matzarakis, A.; Fröhlich, D. Sport events and climate for visitors—The case of FIFA World Cup in Qatar 2022. *Int. J. Biometeorol.* **2015**, *59*, 481–486. [[CrossRef](#)] [[PubMed](#)]
35. Casa, D.J.; DeMartini, J.K.; Bergeron, M.F.; Csillan, D.; Eichner, E.R.; Lopez, R.M.; Ferrara, M.S.; Miller, K.C.; O'Connor, F.; Sawka, M.N. National Athletic Trainers' Association position statement: Exertional heat illnesses. *J. Athl. Train.* **2015**, *50*, 986–1000. [[CrossRef](#)] [[PubMed](#)]
36. Larsen, T.; Kumar, S.; Grimmer, K.; Potter, A.; Farquharson, T.; Sharpe, P. A systematic review of guidelines for the prevention of heat illness in community-based sports participants and officials. *J. Sci. Med. Sport* **2007**, *10*, 11–26. [[CrossRef](#)] [[PubMed](#)]
37. Parsons, K. *Human Thermal Environments: The Effects of Hot, Moderate, and Cold Environments on Human Health, Comfort, and Performance*; CRC Press: Boca Raton, FL, USA, 2014; ISBN 146659599X.
38. Nikolopoulou, M.; Steemers, K. Thermal comfort and psychological adaptation as a guide for designing urban spaces. *Energy Build.* **2003**, *35*, 95–101. [[CrossRef](#)]
39. Thorsson, S.; Lindqvist, M.; Lindqvist, S. Thermal bioclimatic conditions and patterns of behaviour in an urban park in Goteborg, Sweden. *Int. J. Biometeorol.* **2004**, *48*, 149–156. [[CrossRef](#)] [[PubMed](#)]
40. Vanos, J.K.; Warland, J.S.; Gillespie, T.J.; Kenny, N.A. Thermal comfort modelling of body temperature and psychological variations of a human exercising in an outdoor environment. *Int. J. Biometeorol.* **2012**, *56*. [[CrossRef](#)] [[PubMed](#)]
41. Peel, B.L.; Finlayson, B.L.; McMahon, T.A. Updated world map of the Koppen-Geiger climate classification. *Hydrol. Earth Syst. Sci.* **2007**, *11*, 1633–1644. [[CrossRef](#)]
42. Environment and Climate Change Canada. *Climate Change Science and Research*; Government of Canada: Gatineau, QC, Canada, 2016.
43. Penney, J. Climate change adaptation in the city of Toronto: Lessons for Great Lakes Communities. *Clean Air Partnersh.* **2008**.
44. Stewart, I.; Oke, T.R. A New Classification System for Urban Climate Sites. *Bull. Am. Meteorol. Soc.* **2012**, *90*, 922–923.
45. Government of Canada Open Government Portal, Open Data. Available online: <https://open.canada.ca/en/open-data> (accessed on 25 April 2018).
46. Budd, G.M. Wet-bulb globe temperature (WBGT)—Its history and its limitations. *J. Sci. Med. Sport* **2008**, *11*, 20. [[CrossRef](#)] [[PubMed](#)]
47. Armstrong, L.; Casa, D.; Millard-Stafford, M.; Moran, D.; Pyne, S.; Roberts, W. American College of Sports Medicine position stand: Exertional heat illness during training and competition. *Med. Sci. Sport. Exerc.* **2007**, *39*, 556–572. [[CrossRef](#)] [[PubMed](#)]
48. Brown, R.D.; Gillespie, T.J. Estimating outdoor thermal comfort using a cylindrical radiation thermometer and an energy budget model. *Int. J. Biometeorol.* **1986**, *30*, 43–52. [[CrossRef](#)] [[PubMed](#)]
49. Kenny, N.A.; Warland, J.S.; Brown, R.D.; Gillespie, T.G. Part A: Assessing the performance of the COMFA outdoor thermal comfort model on subjects performing physical activity. *Int. J. Biometeorol.* **2009**, *53*, 415–428. [[CrossRef](#)] [[PubMed](#)]
50. Kenny, N.A.; Warland, J.S.; Brown, R.D.; Gillespie, T.J. Part B: Revisions to the COMFA outdoor thermal comfort model for application to subjects performing physical activity. *Int. J. Biometeorol.* **2009**, *53*, 429–441. [[CrossRef](#)] [[PubMed](#)]
51. Grundstein, A.; Knox, J.; Vanos, J.K.; Cooper, E.; Casa, D.J. American Football and Fatal Exertional Heat Stroke: A Case Study of Korey Stringer. *Int. J. Biometeorol.* **2017**, *61*, 1471–1480. [[CrossRef](#)] [[PubMed](#)]
52. Montieth, J.; Unsworth, M. *Principles of Environmental Biophysics*, 3rd ed.; Elsevier: New York, NY, USA, 2008.

53. Kenny, N.A.; Warland, J.S.; Brown, R.D.; Gillespie, T.J. Estimating the radiation absorbed by a human. *Int. J. Biometeorol.* **2008**, *52*, 491–503. [[CrossRef](#)] [[PubMed](#)]
54. Harlan, S.L.; Brazel, A.J.; Prashad, L.; Stefanov, W.L.; Larsen, L. Neighborhood microclimates and vulnerability to heat stress. *Soc. Sci. Med.* **2006**, *63*, 2847–2863. [[CrossRef](#)] [[PubMed](#)]
55. Ainsworth, B.E.; Haskell, W.L.; Herrmann, S.D.; Meckes, N.; Bassett, D.R., Jr.; Tudor-Locke, C.; Greer, J.L.; Vezina, J.; Whitt-Glover, M.C.; Leon, A.S. 2011 Compendium of Physical Activities: A second update of codes and MET values. *Med. Sci. Sports Exerc.* **2011**, *43*, 1575–1581. [[CrossRef](#)] [[PubMed](#)]
56. Vanos, J.; Herdt, A.; Lochbaum, M. Effects of Physical Activity and Shade on the Heat Balance and Thermal Perceptions of Children in a Playground Microclimate. *Build. Environ.* **2017**, *126*, 119–131. [[CrossRef](#)]
57. Strath, S.J.; Swartz, A.M.; Bassett, D.R.; O'Brien, W.L.; King, G.A.; Ainsworth, B.E. Evaluation of heart rate as a method for assessing moderate intensity physical activity. *Med. Sci. Sport Exerc.* **2000**, *32*, S465–S470. [[CrossRef](#)]
58. ISO. *ISO 9920: Ergonomics of the Thermal Environment: Estimation of Thermal Insulation and Water Vapour Resistance of a Clothing Ensemble*; ISO: Geneva, Switzerland, 2007.
59. Luo, F.; Cao, G.; Mulligan, K.; Li, X. Explore spatiotemporal and demographic characteristics of human mobility via Twitter: A case study of Chicago. *Appl. Geogr.* **2016**, *70*, 11–25. [[CrossRef](#)]
60. Jurdak, R.; Zhao, K.; Liu, J.; AbouJaoude, M.; Cameron, M.; Newth, D. Understanding human mobility from Twitter. *PLoS ONE* **2015**, *10*, e0131469. [[CrossRef](#)] [[PubMed](#)]
61. Liu, Y.; Liu, X.; Gao, S.; Gong, L.; Kang, C.; Zhi, Y.; Chi, G.; Shi, L. Social sensing: A new approach to understanding our socioeconomic environments. *Ann. Assoc. Am. Geogr.* **2015**, *105*, 512–530. [[CrossRef](#)]
62. Leetaru, K.; Wang, S.; Cao, G.; Padmanabhan, A.; Shook, E. Mapping the global Twitter heartbeat: The geography of Twitter. *First Monday* **2013**, *18*, 5. [[CrossRef](#)]
63. Demuth, J.L.; Morss, R.E.; Palen, L.; Anderson, K.M.; Anderson, J.; Kogan, M.; Stowe, K.; Bica, M.; Lazrus, H.; Wilhelmi, O. “sometimes da# beachlife ain’t always da wave”: Understanding People’s Evolving Hurricane Risk Communication, Risk Assessments, and Responses Using Twitter Narratives. *Weather Clim. Soc.* **2018**. [[CrossRef](#)]
64. Cao, G.; Wang, S.; Hwang, M.; Padmanabhan, A.; Zhang, Z.; Soltani, K. A scalable framework for spatiotemporal analysis of location-based social media data. *Comput. Environ. Urban Syst.* **2015**, *51*, 70–82. [[CrossRef](#)]
65. Xiao, Y.; Huang, Q.; Wu, K. Understanding social media data for disaster management. *Nat. Hazards* **2015**, *79*, 1663–1679. [[CrossRef](#)]
66. Yin, J.; Lampert, A.; Cameron, M.; Robinson, B.; Power, R. Using social media to enhance emergency situation awareness. *IEEE Intell. Syst.* **2012**, *27*, 52–59. [[CrossRef](#)]
67. Jung, J.; Uejio, C.K. Social media responses to heat waves. *Int. J. Biometeorol.* **2017**, *61*, 1247–1260. [[CrossRef](#)] [[PubMed](#)]
68. Giuffrida, L.M. Assessing the Effect of Weather on Human Outdoor Perception Using Twitter 2017. Ph.D. Thesis, Universidade Nova de Lisboa, Lisbon, Portugal, 2017.
69. Twitter Inc. Twitter Streaming Application Program Interface. Available online: <https://developer.twitter.com/en/docs> (accessed on 20 June 2018).
70. Oke, T.R.; Hannell, F.G. The form of the urban heat island in Hamilton, Canada. *WMO Tech. Note* **1970**, *108*, 113–126.
71. Blair, R. Meteorological Variations and Their Impact on NO₂ Concentrations in the Toronto-Hamilton Urban Air-Shed. Ph.D. Thesis, McMaster University, Hamilton, ON, Canada, 2006.
72. Graham, D.A.; Vanos, J.K.; Kenny, N.A.; Brown, R.D. Modeling the effects of urban design on emergency medical response calls during extreme heat events in Toronto, Canada. *Int. J. Environ. Res. Public Health* **2017**, *14*, 778. [[CrossRef](#)] [[PubMed](#)]
73. Muller, C.L.; Chapman, L.; Grimmond, C.S.B.; Young, D.T.; Cai, X. Sensors and the city: A review of urban meteorological networks. *Int. J. Climatol.* **2013**, *33*, 1585–1600. [[CrossRef](#)]
74. Resch, B.; Mittleboeck, M.; Lipson, S.; Welsh, M.; Bers, J.; Britter, R.; Ratti, C.; Blaschke, T. Integrated Urban Sensing: A Geo-sensor Network for Public Health Monitoring and Beyond. *Int. J. Geogr. Inf. Sci.* **2011**. Available online: <https://dspace.mit.edu/handle/1721.1/64636> (accessed on 20 June 2018).
75. Luber, G.; McGeehin, M. Climate Change and Extreme Heat Events. *Am. J. Prev. Med.* **2008**, *35*, 429–435. [[CrossRef](#)] [[PubMed](#)]

76. Karner, A.; Hondula, D.M.; Vanos, J.K. Heat exposure during non-motorized travel: Implications for transportation policy under climate change. *J. Transp. Health* **2015**, *2*. [[CrossRef](#)]
77. Basara, J.B.; Illston, B.G.; Fiebrich, C.A.; Browder, P.D.; Morgan, C.R.; McCombs, A.; Bostic, J.P.; McPherson, R.A.; Schroeder, A.J.; Crawford, K.C. The Oklahoma city microneet. *Meteorol. Appl.* **2011**, *18*, 252–261. [[CrossRef](#)]
78. Hardin, A.W.; Liu, Y.; Cao, G.; Vanos, J.K. Urban heat island intensity and spatial variability by synoptic weather type in the northeast US. *Urban Clim.* **2017**. [[CrossRef](#)]
79. Anderson, J.E.; Usher, J. Mesonet Programs Needs and Best Practices. In Proceedings of the 10th EMS Annual Meeting, 10th European Conference on Applications of Meteorology (ECAM) Abstracts, Zürich, Switzerland, 13–17 September 2010.
80. Kosaka, E.; Iida, A.; Vanos, J.; Middel, A.; Yokohari, M.; Brown, R. Microclimate variation and estimated heat stress of runners in the 2020 Tokyo Olympic Marathon. *Atmosphere (Basel)* **2018**, *9*, 192. [[CrossRef](#)]
81. Kinney, P.L.; O'Neill, M.S.; Bell, M.L.; Schwartz, J. Approaches for estimating effects of climate change on heat-related deaths: Challenges and opportunities. *Environ. Sci. Policy* **2008**, *11*, 87–96. [[CrossRef](#)]
82. Spagnolo, J.; De Dear, R. A field study of thermal comfort in outdoor and semi-outdoor environments in subtropical Sydney Australia. *Build. Environ.* **2003**, *38*, 721–738. [[CrossRef](#)]
83. Brown, R.D. Ameliorating the effects of climate change: Modifying microclimates through design. *Landsc. Urban Plan.* **2011**, *100*, 372–374. [[CrossRef](#)]
84. Perini, K.; Magliocco, A. Effects of vegetation, urban density, building height, and atmospheric conditions on local temperatures and thermal comfort. *Urban For. Urban Green.* **2014**, *13*, 495–506. [[CrossRef](#)]
85. Hardin, A.W.; Vanos, J.K. The influence of surface type on the absorbed radiation by a human under hot, dry conditions. *Int. J. Biometeorol.* **2018**, *62*, 43–56. [[CrossRef](#)] [[PubMed](#)]
86. Papachristou, C.; Foteinaki, K.; Kazanci, O.B.; Olesen, B.W. Structures that Include a Semi-Outdoor Space: Part 2: Thermal Environment. In Proceedings of the 12th REHVA World Congress, Aalborg, Denmark, 22–25 May 2016.
87. Bouyer, J.; Vinet, J.; Delpech, P.; Carre, S. Thermal comfort assessment in semi-outdoor environments: Application to comfort study in Stadia. *J. Wind Eng. Ind. Aerodyn.* **2007**, *95*, 963–976. [[CrossRef](#)]
88. Middel, A.; Lukaszczuk, J.; Maciejewski, R. Sky View Factors from synthetic fisheye photos for thermal comfort routing—A case study in phoenix, Arizona. *Urban Plan.* **2017**, *2*, 19–31. [[CrossRef](#)]
89. Dolney, T.J.; Sheridan, S.C. The relationship between extreme heat and ambulance response calls for the city of Toronto, Ontario, Canada. *Environ. Res.* **2006**, *101*, 94–103. [[CrossRef](#)] [[PubMed](#)]
90. Hosokawa, Y.; Grundstein, A.J.; Vanos, J.K.; Cooper, E.R. Environmental Condition and Monitoring. In *Sport and Physical Activity in the Heat*; Springer: Berlin, Germany, 2018; pp. 147–162.
91. Sofotasiou, P.; Hughes, B.R.; Calautit, J.K. Qatar 2022: Facing the FIFA World Cup climatic and legacy challenges. *Sustain. Cities Soc.* **2015**, *14*, 16–30. [[CrossRef](#)]
92. Tsunematsu, N.; Yokoyama, H.; Honjo, T.; Ichihashi, A.; Ando, H.; Shigyo, N. Relationship between land use variations and spatiotemporal changes in amounts of thermal infrared energy emitted from urban surfaces in downtown Tokyo on hot summer days. *Urban Clim.* **2016**, *17*, 67–79. [[CrossRef](#)]
93. Schuster, C.; Honold, J.; Lauf, S.; Lakes, T. Urban heat stress: Novel survey suggests health and fitness as future avenue for research and adaptation strategies. *Environ. Res. Lett.* **2017**, *12*, 44021. [[CrossRef](#)]
94. Périard, J.D.; Racinais, S.; Sawka, M.N. Adaptations and mechanisms of human heat acclimation: Applications for competitive athletes and sports. *Scand. J. Med. Sci. Sports* **2015**, *25*, 20–38. [[CrossRef](#)] [[PubMed](#)]
95. Havenith, G.; van Middendorp, H. The relative influence of physical fitness, acclimatization state, anthropometric measures and gender on individual reactions to heat stress. *Eur. J. Appl. Physiol. Occup. Physiol.* **1990**, *61*, 419–427. [[CrossRef](#)] [[PubMed](#)]

